Biophysical Chemistry, 37 (1990) 61–71
Elsevier

BIOCHE 01465

Perturbation of molecular species distribution in steady states supported by a flow of energy

Models analogous to Ca^{2+}-dependent ATPase and phosphorylase *b*

Enrico Bucci and Robert F. Steiner

Department of Biochemistry, University of Maryland Medical School, 660 W. Redwood St, Baltimore, MD 21201 and Department of Chemistry, University of Maryland Baltimore County, Wilkens Ave, Catonsville, MD 21228, U.S.A.

Received 12 December 1989
Accepted 1 February 1990

Ca^{2+} transport; Phosphorylase *b*; Pseudoequilibrium; Cooperativity; Binding model; Steady state

When an allosteric macromolecular system is capable of existing in two conformations, both of which may be converted into energy-storing forms by the binding of a substrate or by the absorption of radiant energy, then a kinetic process may occur, such as an enzymic conversion of the substrate into products, which liberates energy and selectively depletes one or more of the forms of the macromolecule. Upon a continuous supply of energy, a steady state, or pseudoequilibrium, is reached during which the selective depletion of molecular species results effectively in a directional flow of energy through the system. This perturbs the distribution of the various molecular species. This effect may simulate both positive and negative binding cooperativity, and mimic the presence of multiple binding sites with different affinities even in monomeric, monovalent systems. Specific model systems are presented analogous to the transport of Ca^{2+} by sarcoplasmic reticulum and the allosteric behavior of phosphorylase *b*.

1. Introduction

Macromolecular systems of biological relevance are often found in multiple conformations and/or aggregation states, upon which depends their biological activity. These systems are commonly defined as allosteric.

The kinetics of ligand binding and product release by allosteric systems often yield steady states, for which there is no change with time of the relative proportions of the various molecular species although the distribution of species does not correspond to equilibrium. In fact, their distribution is altered by a rearrangement of the kinetics of transformation of the species into each other, supported by a flow of energy through the system, as produced by the degradation of ligands into products. These thermokinetic phenomena are here defined as pseudoequilibria, since, in contrast to equilibria, they are characterized by a free energy change in time different from zero, i.e., $\Delta G \neq 0$.

In these systems, we can distinguish resting forms, in the absence of ligands, and activated forms, which bind substrates/ligands and are responsible for their degradation *.

The thermokinetic behavior of these systems has been thoroughly analyzed by Hill [1] and Walz and Caplan [2,3]. Their analyses have clearly described the nature of the distribution of energy for various models of these systems.

In this paper, we have considered the effect of

Correspondence address: E. Bucci, Department of Biochemistry, University of Maryland Medical School, 660 W. Redwood St, Baltimore, MD 21201, U.S.A.

* It should be noted that if the activated forms release their ligands unchanged, without formation of products, no flow of energy is produced and a true equilibrium is established.

0301-4622/90/$03.50 © 1990 Elsevier Science Publishers B.V. (Biomedical Division)

pseudoequilibria on phenomenological parameters, as obtained from ligand-binding isotherms, which are typically the basis for the interpretation of the molecular mechanism of allosteric transitions. We demonstrate that kinetic factors may mold the saturation curves into a variety of shapes, simulating molecular models which may not exist.

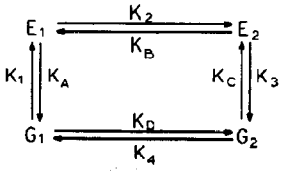

Fig. 1. Square model which is at the basis of all other simulations. The E forms are ligand bound; the G forms are ligand-free.

2. Single systems

Let us consider an enzymatic reaction where an enzyme in the resting state, G_1, reacts with a ligand (substrate), L, producing an activated form, the complex, E_1, which releases the product, P. These events can be represented by

$$G_1 + L \underset{K_A}{\overset{K_1}{\rightleftarrows}} E_1 \xrightarrow{K_F} P + G_1 \qquad (1)$$

In the absence of product formation, the equilibrium constant for formation of the complex E_1 is defined by $K_E = K_1/K_A$. When products are formed the net rate constant for formation of G_1 becomes $K'_A = K_A + K_F$, and the pseudoequilibrium is described by $K_P = K_1/K'_A$. Clearly, $K_E > K_P$, because the release of products prevents accumulation of the complex E_1. When products are formed, in order to reach a steady state with maximum saturation of the enzyme by the substrate (i.e., when 100% of the system is E_1), a higher ligand concentration is required. The saturation curve, as measured by the fractional increase in the rate of reaction until a maximal velocity is reached, will still be the classic Michaelis-Menten hyperbola. The energy cost of the pseudoequilibrium is

$$\Delta G_{extra} = -RT \ln(K_E/K_P) \qquad (2)$$

and is provided by the degradation of the substrates/ligands into products.

3. Polymorphic systems

These systems are characterized by a resting state distributed over several resting forms (G), and an activated state characterized by the presence of activated forms (E), namely, complexes of the macromolecules with ligands.

3.1. The square model

The simplest system is shown in fig. 1, where two G forms are in equilibrium with two respective E forms. The various forms relax into one another through single-step transitions. The kinetic constants of the transitions are defined as K_1–K_4 in the clockwise direction, and K_D–K_A counterclockwise. In this way, K_1–K_4 have the counterparts K_D–K_A, respectively. The kinetic constants also define equilibrium constants:

$$\begin{aligned} &Q_1 = K_1/K_A, \\ &Q_2 = K_2/K_B, \\ &Q_3 = K_3/K_C \\ &\text{and} \\ &Q_4 = K_4/K_D. \end{aligned} \qquad (3)$$

The condition for a true thermodynamic equilibrium of the system is that, in going from one species to another, the same amount of energy is consumed on progressing in either the clockwise or counterclockwise direction around the square. Therefore, the following expression must be valid:

$$Q_1Q_2Q_3Q_4 = 1 \qquad (4)$$

Eq. 3 also implies that the product of the clockwise kinetic constants, Π_+, is equal to that of the counterclockwise kinetic constants, Π_-,

$$K_1K_2K_3K_4 = \Pi_+ = \Pi_- = K_AK_BK_CK_D \qquad (5)$$

At equilibrium there is no net change in the various components. Therefore, designating the various molecular species as X_i and the various

rate constants as K_j, for each molecular species we have

$$\frac{dX_i}{dt} = \sum_j K_{ij} X_i = 0 \qquad (6)$$

The solution of these simultaneous equations, for obtaining the quantities X_i as functions of the various rate constants, has been exhaustively discussed by Wyman [4]. A simple computer program based on the evaluation of the proper determinants yields the values of the relative amounts of the four molecular species, namely, G_1 and G_2 (resting forms), and E_1 and E_2 (activated forms). The overall fractional saturation with ligand, Y, is expressed as

$$Y = (E_1 + E_2)/(E_1 + E_2 + G_1 + G_2) \qquad (7)$$

and the fraction of each species (e.g., F_{E_1} for the E_1 species) is defined by

$$F_{E_1} = E_1/(E_1 + E_2 + G_1 + G_2) \qquad (8)$$

From the quantities Y it is possible to compute the Hill coefficient as the slope of the plot of $\log Y/(1-Y)$ vs $\log L$, where L is the free ligand concentration for these quantities.

It should be noted that in the model, constants K_1 and K_C are the pseudo-first-order rate constants of ligand binding. Therefore, their operational value is affected by the amount of free ligand, L, as in

$$K_1' = K_1 L$$
$$K_C' = K_C L \qquad (9)$$

This allows us to simulate titrations with increasing concentrations of ligands.

In order to simplify the notation, the prime has been omitted in the rest of this paper.

3.2. Test of the square model for a true equilibrium

Fig. 2 shows the binding isotherm obtained when the kinetic constants are taken as being all equal to 1 arbitrary unit. As discussed above, in this model we have $\Pi_+ = \Pi_-$, as in a true equilibrium. The amount of ligand (L), also in arbitrary units, is increased until the macromolecule is totally saturated. Solution of eq. 6 is performed at each discrete ligand concentration in order to compute the values of the quantities in eqs 7 and 8.

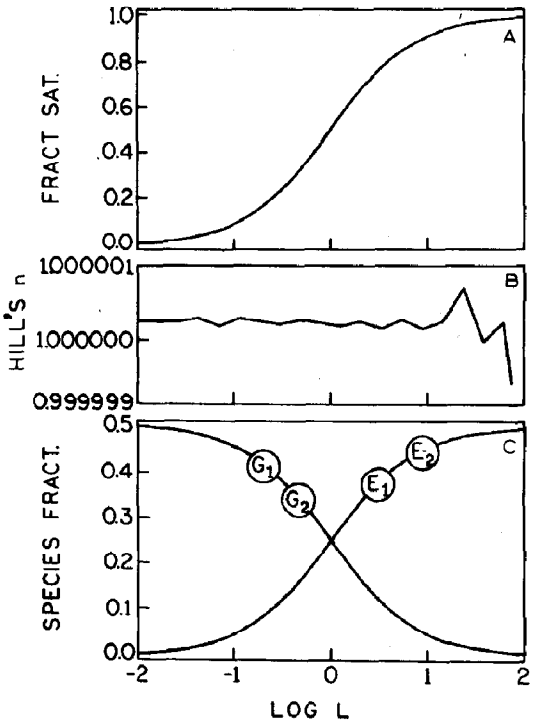

Fig. 2. Equilibrium of binding of the species in the square model with a ligand in the absence of product formation. (A) Overall saturation curve, (B) value of the Hill coefficient n at each point of the saturation curve, (C) modifications of the relative amounts of each species at each point of the saturation curve. All rate constants have unit value.

The result is a hyperbolic binding curve (sigmoidal in the semilogarithmic plot of fig. 2A). The value of the parameter n of the Hill plot is equal to 1.0 throughout the entire saturation curve as shown in fig. 2B. As expected from the identical values of the kinetic constants, the distribution of molecular species at each level of saturation (shown in fig. 2C) is symmetrical, i.e., the binding is equally distributed between the E_1 and E_2 species, whose respective saturation curves are superimposable. Also, G_1 and G_2 progressively disappear in a superimposable fashion.

The kinetic constants in fig. 2 can be varied at will in any possible arbitrary way. Provided that the behavior accords with eqs 2 and 3, the overall binding curve and the variation in the Hill coeffi-

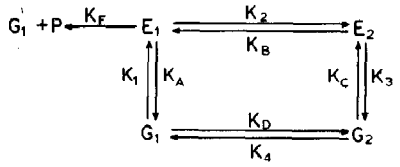

Fig. 3. Perturbation of the square model when E_1 forms products and reverts to its resting form G_1.

cient n remain identical to those shown in fig. 2A and B, except for scale factors on the abscissa. The relative proportions of the various species will vary according to the chosen values of the rate constants. Irrespective of the species distributions, the value of n for the Hill plots will remain equal to 1.0 at each step of the saturation curve, thus demonstrating the hyperbolic shape of the binding isotherm.

3.3. Perturbations leading to a pseudoequilibrium

If the E forms result from the binding of substrate (or from absorption of external energy), the subsequent formation of released products may alter the operational value of one or more of the various kinetic constants, so that the conditions defined in eqs 4 and 5 are not fulfilled. In the square model of fig. 1 two basic mechanisms are possible.

3.3.1. One-step conversion of ligands / substrates

If only one of the E forms is capable of releasing products, we can combine the square model of fig. 1 with eq. 1 to obtain the model outlined in fig. 3. As discussed, the net effect of the conversion by E_1 on the steady state of the square model is an increase in the apparent value of K_A which becomes $K'_A = K_A + K_F$. The consequence is that $\Pi_+ \neq \Pi_-$ and a pseudoequilibrium is established. Analogous reasoning can be applied to the effect of product formation by E_2. In this case, K_3 is the rate constant which apparently increases.

It should be stressed that in this model the conversion is supposed to occur as a one-step process during which either E_1 reverts into G_1 or E_2 reverts into G_2. There is no free energy change in the $E_1 \rightarrow E_2$ transition ($Q_2 = 1$).

In the model of fig. 3, the depletion of E_1, due to the formation of products, forces the system into accumulating G_1, thereby driving the relaxation processes of the system along a counterclockwise direction. In other words, the pseudoequilibrium stabilizes a directional relaxation of the species.

3.3.2. Two-step conversion of ligands / substrates

It may occur that E_1 and E_2 are at significantly different energy levels ($Q_2 \neq 1$). Let us suppose that the excess energy absorbed by E_1 is partially released for forming E_2 before being totally released as products so as to form the resting state G_2. In terms of the model of fig. 1, the rate constant which is increased by product formation is K_3, so that $\Pi_+ \neq \Pi_-$ and a pseudoequilibrium is established. The thermokinetic behavior of the system drives its accumulation of G_2 and the consequent relaxation in a clockwise direction. Alternatively, E_1 can also decay into G_1 and products, increasing the apparent value of K_A and driving the system in a counterclockwise direction. The system will be maximally stabilized by progression along the route which produces the largest energy decay.

A symmetrical and opposite situation is produced when E_2 is the activated species which relaxes into E_1, that forms products.

3.4. Numerical simulations of pseudoequilibria involving one-step conversion

3.4.1. Model a: False negative cooperativity

Starting from the model of fig. 1, which is a true equilibrium, if E_1 becomes a product-forming species as in fig. 3, we can insert $K_A = 10^4$ in the square model, all other constants remaining at unit value. At steady state, the overall saturation curve of the enzyme, which can be measured by the fractional increases in the initial velocity of product formation, will be that shown in fig. 4A. The enzyme appears to bind the substrate at substrate concentrations within two different ranges of values, as if there were two distinct binding sites on the protein, of high and low affinity, respectively. The Hill coefficient, n (fig. 4B), is equal to 1.0 for the two binding events, whereas it falls to a value near zero in the intermediate region. This system would mimic either polyvalent

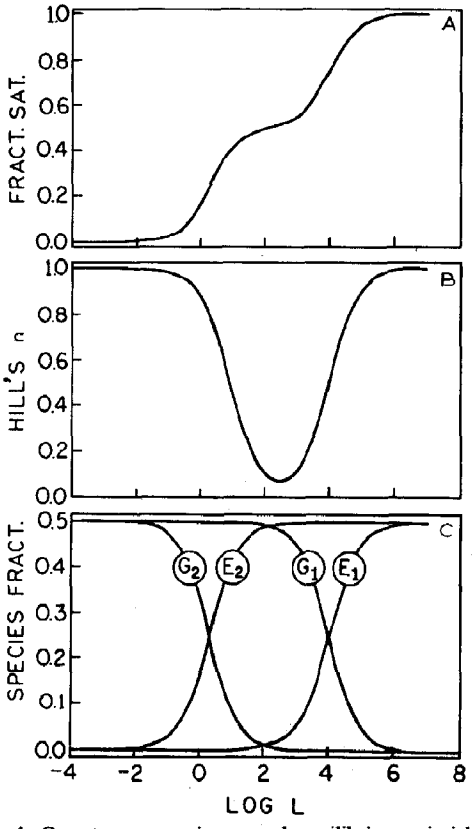

Fig. 4. One-step conversion pseudoequilibrium mimicking a polyvalent binding with negative cooperativity. (A) Overall saturation curve, (B) value of the Hill coefficient n at each point of the saturation curve, (C) modifications of the relative amounts of each species at each point of the saturation curve. $K_A = 10^4$; all other rate constants have unit value.

binding with strong negative cooperativity, or a system with two binding sites of very different binding affinities, even if the system were in reality monovalent. Fig. 4C shows plots which provide support for the existence of two binding events: the directional flow of energy produces a redistribution of the species, which forces the saturation of E_1 and E_2 into different regions of ligand concentration. It should be noted that in fig. 4 the plateau is near the 50% saturation mark, suggesting the presence of two binding sites. By slightly rearranging the rate constants, it is possible to displace the plateau at different saturation levels. Hence, plateaus near the 75 or 25% saturation level are indicative of the presence of four binding sites, three of which have very similar binding properties.

Identical data are obtained when E_2 is the product-forming species so that $K_3 = 10^4$ can be introduced into the model of fig. 1. The only difference is in fig. 4C, where the curves for saturation of E_1 and E_2 and disappearance of G_1 and G_2 are interchanged.

3.4.2. Model b: False positive cooperativity

Consider a system where the most stable forms are G_1 and E_2. In the absence of energy degradation, this situation can be simulated by taking $K_2 = K_4 = 10^3$ and $K_A = K_C = 10^3$ in the square

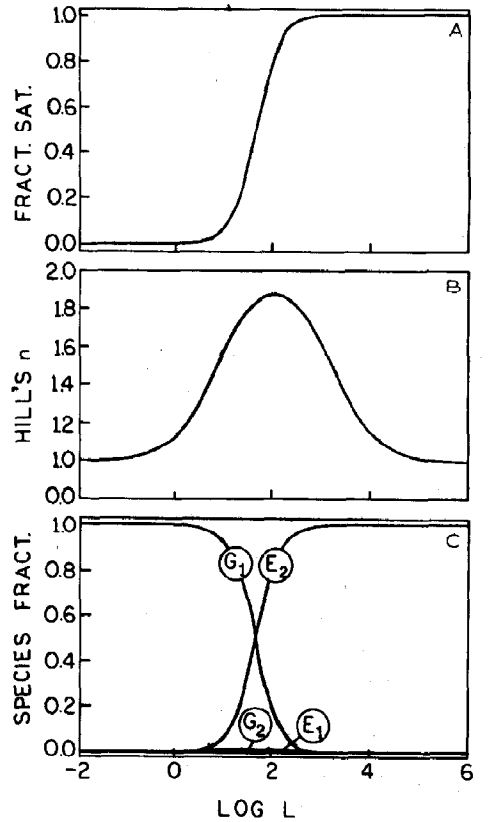

Fig. 5. One-step conversion pseudoequilibrium mimicking polyvalent binding with positive cooperativity. (A) Overall saturation curve, (B) value of the Hill coefficient n at each point of the saturation curve, (C) modifications of the relative amounts of each species at each point of the saturation curve. $K_2 = K_3 = K_4 = K_A = K_C = 10^3$; all other constants have unit value.

model of fig. 1. In this system $\Pi_+ = \Pi_-$, therefore, it will result in an equilibrium like that shown in fig. 2A. Now, suppose that only E_2 can release energy or form products so that the actual value of K_3 in the model is increased to $K_3 = 10^3$. Fig. 5 shows that this system simulates a substrate binding cooperativity with a value for the Hill coefficient n as high as 1.8. This saturation curve suggests the presence of a polymeric system with positive binding cooperativity, even for a monomeric, monovalent system. The false cooperativity is due to product formation which prevents accumulation of the intermediate forms E_1 and G_2, as shown in fig. 5 where they are practically absent at all levels of saturation. It should be stressed that if the value of K_3 is progressively increased beyond 10^3, the positive cooperativity decreases and eventually negative cooperativity similar to that of model a (section 3.4.1.) is produced.

A similar model can be construed by assuming that G_2 and E_1 are the most stable conformations of the system.

3.5. Numerical simulations of pseudoequilibria involving two-step conversions

3.5.1. Model c: Enrichment of unstable resting forms

This model is especially applicable to systems where the rates of binding of ligands (or of absorption and release of energy) are much faster than those of conformational changes in macromolecules. Possible examples of the latter kind include fluorescent systems where radiative energy is absorbed and released on time scales two or more orders of magnitude faster than that of conformational changes of macromolecules.

Suppose we have a system where the resting state is characterized by two conformations G_1 and G_2, of which G_1 is largely preferred because in the square model of fig. 1 $K_D = 10^{-1}$ while $K_4 = 1.0$. Both G_1 and G_2 can bind ligand (or absorb energy) at similar rates, so that $K_1 = K_C = 10^3$, to form E_1 and E_2, respectively. Both E_1 and E_2 release products, reverting into G_1 and G_2, respectively; however, E_1 is at a higher energy level than E_2 and therefore can also decay into E_2. The decays of E_1 into G_1 and of E_2 into G_2 are characterized by similar rates, so that $K_A = K_3 = 10^3$. The transition of E_1 into E_2 occurs at a rate $K_2 = 10^3$ similar to that of all other decays. The different energy level impedes the transformation of E_2 into E_1, therefore the rate K_B can remain at the value $K_B = 1.0$. Inserting these values into the model, at the steady state we have the pseudoequilibrium described by fig. 6.

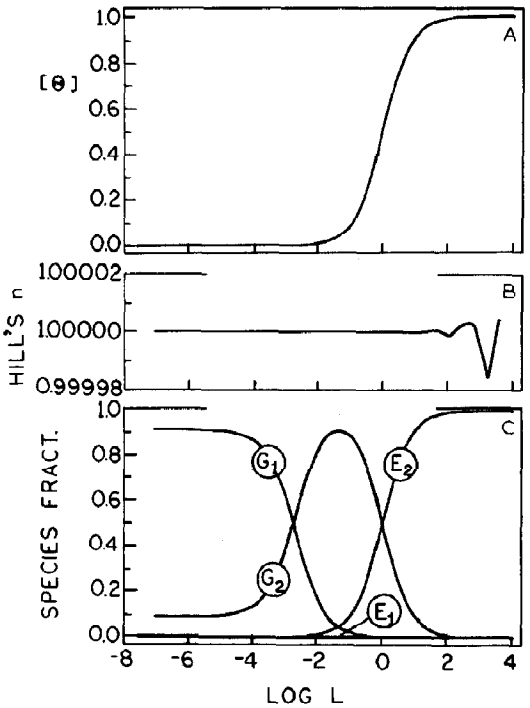

Fig. 6. Two-step pseudoequilibrium. (A) Overall saturation curve, (B) value of the Hill coefficient n at each point of the saturation curve, (C) modifications of the relative amounts of each species at each point of the saturation curve. $K_1 = K_2 = K_3 = K_A = K_C = 10^3$, $K_D = 0.1$; all other constants have unit value. θ: fraction of maximum binding of ligand or absorption of external energy.

Fig. 6 is very instructive and the distribution of molecular species is unexpected. Species E_1 is never formed, and E_2 (i.e., the only form which saturates with ligands) begins to form only when all of the system is practically in the G_2 conformation. Moreover, G_1 is quantitatively transformed into G_2 when minimal amounts of ligands (or of energy) are absorbed by the system into practically undetectable amounts of E_1 and E_2. It should be emphasized that G_2 is largely a minor compo-

nent of the system in the absence of ligands or irradiation. However, the whole system is transformed into G_2 merely upon negligible saturation of the system. This implies a redistribution of the species which stabilizes ligand-free forms that practically do not exist in the absence of external, product-forming, ligands.

The accumulation of G_2 is a consequence of the low rates chosen for K_B and K_4. If species E_2 and G_2 are allowed to undergo faster transformations into E_1 and G_1, respectively, the amount of stabilization of the resting form G_2 decreases and eventually disappears.

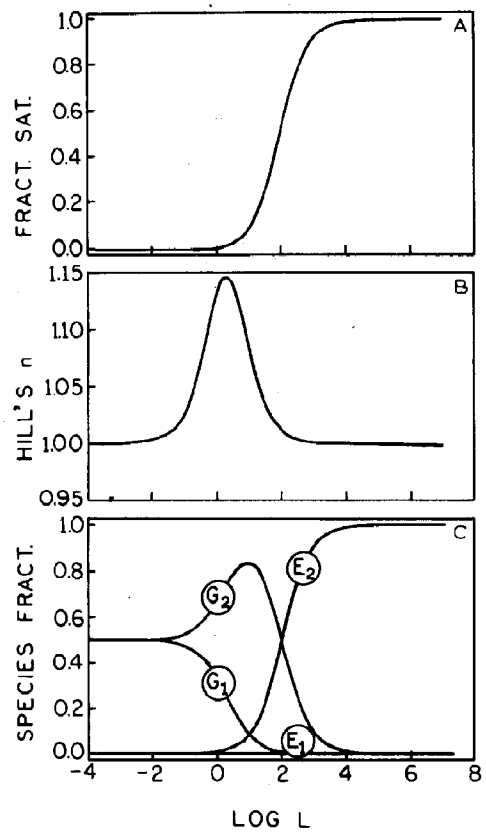

Fig. 7. Two-step conversion pseudoequilibrium involving a chemical substrate. (A) Overall saturation curve, (B) value of the Hill coefficient n at each point of the saturation curve, (C) modifications of the relative amounts of each species at each point of the saturation curve. $K_2 = K_C = 10^3$, $K_3 = 10^5$; all other constants have unit value.

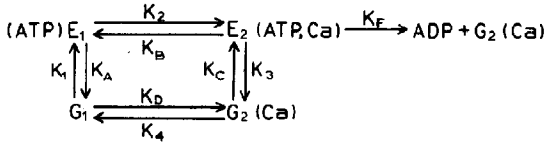

Fig. 8. Square model simulating an activity analogous to that of Ca^{2+}-dependent ATPase.

3.5.2. *Model d: The false single species*

It is a common phenomenon in allosteric systems that ligand binds preferentially to selected conformations of the macromolecule. This model can be simulated by introducing into the square model $K_2 = 10^3$ and $K_C = 10^3$. Under these conditions, eqns 2 and 3 are obeyed and the system is in perfect thermodynamic equilibrium. Product formation by the species E_2, the favored species upon substrate binding, can be simulated by introducing $K_3 = 10^5$ in the model mentioned above. Fig. 7 shows the results in the case of the steady state. The species distribution in fig. 7C shows that the whole system is extensively displaced toward the G_2 form when the absorption of substrate, with consequent product formation, is still negligible. Also, the overall binding curve shows a localized positive cooperativity that is scarcely detectable by the experimenter. In fact, the value of the Hill coefficient n increases only to 1.15, and solely below 2% saturation of the system with ligand. Above this level of saturation, the value of n remains constant at unity, suggesting hyperbolic binding. It should be noted that increasing the value of K_3 to 10^8 produces a localized negative cooperativity with a value of $n = 0.6$. This phenomenon is still undetectable as it occurs below 2% saturation of the system.

Thus, while in the absence of substrate the system is equally distributed between the forms G_1 and G_2, in the presence of negligible amounts of substrate it is quantitatively transformed into G_2, mimicking a system with a single resting species. This model is the counterpart for enzymatic systems of model c (section 3.5.1). In addition, in this case product formation is associated with a flow of energy through the system which stabilizes unstable resting conformations.

Table 1

Values of the rate constants in the square model of fig. 9 for the activity of Ca^{2+}-dependent ATPase

The monomolecular rates are given in s^{-1}. The ligands whose concentrations affect pseudo-first-order rates are indicated within square brackets. The numerical values of the pseudo-first-order constants are inferred from the data reported by Inesi et al. [5], converted to units of $\mu M^{-1} s^{-1}$.

$K_1 = 10.0$ [ATP]	$K_A = 20$
$K_2 = 1.0$ [Ca^{2+}]	$K_B = 30$
$K_3 = 500$	$K_C = 0.01$ [ATP]
$K_4 = 30$	$K_D = 10.0$ [Ca^{2+}]

4. Applications to experimental systems

4.1. Model e: Transport systems analogous to Ca^{2+}-dependent ATPase

Ca^{2+}-dependent ATPase is a complex macromolecular system whose biological function is the transport of Ca^{2+} across the membrane of the sarcoplasmic reticulum of muscle. Based on the review by Inesi et al. [5], the coupling between ATP degradation and Ca^{2+} transport can be represented in oversimplified form by the square model of fig. 8. In the model, several subsequent conformational changes have been collected into single-step transitions, taking the lowest, and thereby limiting, conversion rate as the rate of the entire process.

In the model, G_1 is the free enzyme, G_2 binds both Ca^{2+} and P_i, E_1 binds ATP, and E_2 binds simultaneously ATP and Ca^{2+}. E_2 is the only active form of the enzyme which hydrolyses ATP to form ADP and G_2. G_2 releases Ca^{2+} and reverts into the free enzyme G_1 *. A clockwise cycle is the calcium pump, where the Ca^{2+} absorbed in the E_1-to-E_2 transition is released by the G_2-to-G_1 relaxation.

Table 1 lists the values assigned to the various kinetic constants, as suggested by the schematic proposed in the review. All constants are expressed in units of s^{-1}, the pseudo-first-order constants expressing the rate of binding of either ATP or Ca^{2+} being given in units of the concentration experimentally used for the various ligands ($\mu M^{-1} s^{-1}$). These rates are modified by the concentration of the respective ligand, as indicated within square brackets beside the value of the constants.

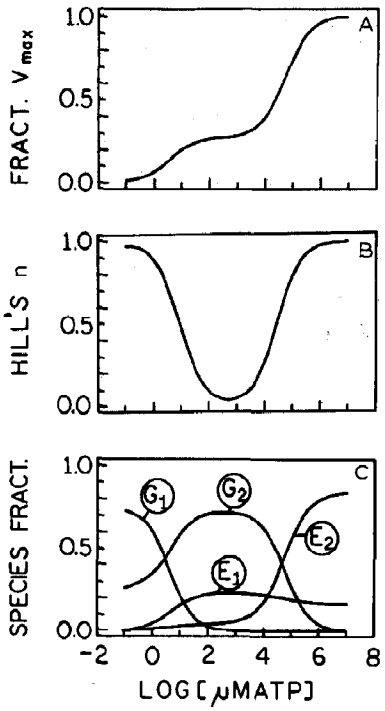

Fig. 9. Simulation of the activity of a model analogous to Ca^{2+}-ATPase based on the square model of fig. 8 and the constants listed in table 1. The system is titrated with ATP; free [Ca^{2+}] = 0.1 mM. Fractional saturation represented as the fractional maximum velocity of the hydrolysis of ATP. (A) Overall saturation curve, (B) value of the Hill coefficient n at each point of the saturation curve, (C) modifications of the relative amounts of each species at each point of the saturation curve.

It should be noted that the schematic in the review of Inesi et al. [5] did not include the rate which could be assigned in our model to K_C. The rate reported in the review is the net rate for the formation of species G_2 from E_2, viz., $K_3 + K_F - K_C$. On this basis, a very low numerical value was assigned to K_C, while those for $K_3 + K_F$ were the rates given in the review. Simulations were performed at various fixed concentrations of Ca^{2+} which define the operational values of the con-

* The species G_2 also releases P_i in the real system. It is a final product of the hydrolysis of ATP, with much lower affinity for any of the forms of the cycles than Ca^{2+} or ATP. A discussion of its effects is beyond the scope of this presentation.

stants K_2 and K_D. The system was titrated with increasing amounts of ATP. A typical simulation is shown in fig. 9, at $[Ca^{2+}] = 0.1$ M.

It should also be borne in mind that the species E_2 and G_2 are those with the highest affinity for Ca^{2+}. Thus, in the presence of Ca^{2+}, these are the most stable conformations of the system. The conversion of substrate forces the relaxations of the various species along a clockwise direction. In order to complete the cycle, E_2 is forced to relax into G_2 and G_2 into G_1, even in the presence of free Ca^{2+}. These forced relaxations represent the calcium pump.

The overall saturation curve with ATP is expressed by the fractional maximum velocity of the hydrolysis. Fig. 9A shows that the system defines a false negative cooperativity as discussed above for model a. The saturation curve is biphasic, mimicking the presence of low- and high-affinity binding sites for ATP. It is intriguing to observe that this simulation is qualitatively consistent with the experimental data for the real system, in spite of the oversimplified nature of the model. Commonly, the plateau is taken as a demonstration of the complete saturation of active sites of the enzyme with ATP, followed by subsequent binding of ATP to a regulatory site, which further increases the speed of the reaction. At the intermediate plateau, the stoichiometry of Ca^{2+} transported to ATP hydrolysed is 2:1. This is the origin of the hypothesis that each subunit has two binding sites for Ca^{2+} and one hydrolytic site for ATP.

Our simulations show that the proposal of a second regulatory binding site for ATP may not be necessary and suggest a speculative alternative model for Ca^{2+} transport. The functional unit of the enzyme could be a homodimer in which each subunit binds one Ca^{2+} and one ATP. Cooperative phenomena regulate the binding and release of Ca^{2+} from the dimer, so that binding and hydrolysis of only one ATP per dimer produces total saturation and desaturation, respectively, of the dimer with Ca^{2+}. Higher concentrations of ATP will eventually saturate all of the hydrolytic sites, thereby increasing the rate of hydrolysis as shown in the simulation, as if ATP were binding to a second regulatory site.

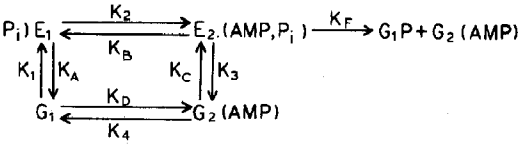

Fig. 10. Square model simulating an activity analogous to that of phosphorylase *b*. G_1P, glucose 1-phosphate.

This model can be tested. If correct, one should observe the occurrence of cooperative phenomena in the binding of calcium, and the approach to a value of 1:1 for the stoichiometry of Ca^{2+} transported to ATP hydrolyzed at high ATP concentrations. The presence of cooperative binding of Ca^{2+} has been demonstrated [5]. The stoichiometry of Ca^{2+} transport for complete saturation of the enzyme with ATP is uncertain.

4.2. Model f: Allosteric systems analogous to phosphorylase b

Glycogen phosphorylase *b* is a classic example of an allosteric system which catalyzes the conversion of glycogen into glucose 1-phosphate. In the presence of the allosteric modifier AMP, the enzyme adopts an active conformation [6,7]. The enzyme is a dimer of identical subunits so tightly bound to each other, that it may be considered a single molecule. Each subunit binds simultaneously glycogen, AMP and P_i, in order to give rise to hydrolysis. Relevant functional characteristics of the system are binding cooperativity of AMP and cooperative binding of the substrate P_i, as monitored by the fractional maximum velocity of phosphorolysis. Notably, the extent of this last cooperativity, as monitored by the value of n for the Hill plots, varies inversely with AMP concentration, until disappearing [6–10].

If the enzyme is assumed to be saturated with glycogen, a model preserving the primary features of the overall process can again be condensed into the square model of Fig. 10. In this scheme, G_1 is the free enzyme, G_2 binds AMP, E_1 binds P_i and E_2 binds both P_i and AMP. Only E_2 produces glucose 1-phosphate. Simulations are performed assuming fixed concentrations of AMP while the system is titrated with P_i.

Table 2

Values of the rate constants used in the square model of fig. 10 for the activity of phosphorylase *b*

The monomolecular rates are given in s^{-1}. The ligands whose concentrations affect pseudo-first-order rates are shown within square brackets. These pseudo-first-order constants are inferred from available data [6–10] expressed as $mM^{-1}\ s^{-1}$.

$K_1 = 10\ [P_i]$	$K_A = 1$
$K_2 = 10^4\ [AMP]$	$K_B = 1$
$K_3 = 2 \times 10^3$	$K_C = 10^3\ [P_i]$
$K_4 = 10^4$	$K_D = 1\ [AMP]$

The only rate constant for which a literature value is available is the rate of phosphorolysis: 10^3 $M^{-1}\ s^{-1}$ [6]. Equilibrium constants have also been measured, however, the data have been obtained during enzyme activity, and therefore are distorted by the flow of energy occurring in the system. The only exception is the equilibrium constant which in terms of the model in fig. 1 is $K_1/K_A = 10.0$ [10].

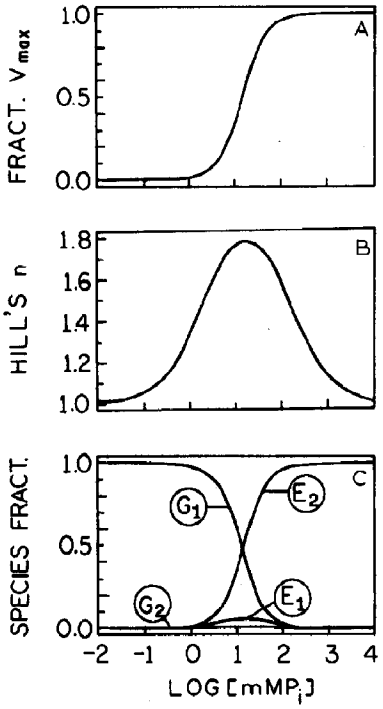

Fig. 11. Simulation of the activity of a model analogous to phosphorylase *b* using the square model of fig. 10. The enzyme is assumed to be always saturated with glycogen. [AMP] = 1.0 mM. The system is titrated with P_i. Fractional saturation with P_i given as the fractional maximum velocity of hydrolysis. (A) Overall saturation curve, (B) value of the Hill coefficient *n* at each point of the saturation curve, (C) modifications of the relative amounts of each species at each point of the saturation curve.

Table 2 lists the numerical values for the rates of the model in fig. 10 as reconstructed on the basis of the incomplete data available from the literature. Also in this case we have taken the experimental value of the rate of phosphorolysis as being inclusive of the back reactions, $K_3 + K_F - K_C$. The available data also support the hypothesis that in the presence of phosphates E_1 has a higher affinity for AMP than G_1. For this reason we assigned a low value to K_2.

Fig. 11 shows that at steady state, the increase in fractional maximum velocity upon titration with P_i was cooperative in behavior with a value of *n* in the Hill plots approaching a peak of 2.0. This is qualitatively consistent with the experimental data. It should be stressed that the level of cooperativity was inversely proportional to the numerical value of K_D. The effective rate of K_D is regulated by the concentration of AMP. This predicts that, on increasing the concentration of AMP in the experimental system the cooperativity would decrease and eventually disappear. Indeed, one of the characteristics of phosphorylase *b* is the inverse relationship between cooperativity and AMP concentration.

Both the cooperativity and the effect of AMP on cooperativity have already been explained on the basis of the allosteric behavior of the enzyme. The model here proposed is still allosteric and adds to the old model new hypotheses regarding the sequence of events which take place during the enzymatic activity.

5. Discussion

In the models here presented, we did not include multisubunit systems in which association-dissociation phenomena contribute to the conformational changes. Such systems will be regulated not only by ligand binding and degradation, but also by the concentration of the macromolecule.

Table 3

Energy cost of the pseudoequilibria considered for the various models

Model	Energy cost (kcal/mol ligand)
(a) Negative cooperativity	5.5
(b) Positive cooperativity	4.1
(c) Enrichment	5.5
(d) False single	6.8
(e) Ca^{2+} ATPase	8.9
(f) Phosphorylase *b*	11.2

Many other models can certainly be conceived and explored, besides those proposed here. As seen in the models analogous to the Ca^{2+} transport and glycogen phosphorolysis systems, the simple square model shown in fig. 1 is quite flexible and can be adapted to fit a variety of circumstances even involving a multiplicity of ligands. We leave this responsibility to our readers with two considerations. Pseudoequilibria are degenerate in the sense that many different combinations of parameters will give similar data. By changing the parameters at random, most frequently negative cooperativity is produced. Also, in order to avoid losing contact with reality, it is a good procedure to start from equilibrium models which are then perturbed by substrate conversion, as performed in the current article.

The few examples here illustrated demonstrate how useful it is to consider the presence of a flow of energy into any macromolecular system capable of conformational changes. They also imply that once an enzymatic system has been recognized as allosteric, the interpretation of molecular mechanisms based on measurements of fractional maximal velocity should be made very cautiously.

Models c and d introduce an additional caveat. They show that unstable resting forms of the system can be stabilized by pseudoequilibria at very low levels of ligand saturation, where the activity of the system is hardly detectable by the experimenter.

A most important characteristic of pseudoequilibria is the effect on the reversibility of the species involved in single transition steps. There is the establishment of a direction of the various relaxations which implies a precise order of events. Reversibility is accomplished only upon completion of the cycle of transformation. This has far-reaching consequences in biological systems, as is evident in the model for Ca^{2+} transport.

At constant enthalpy, the energy cost of this vectorial ordering is entropic in nature and can be readily estimated: $\Delta G_{extra} = -RT\,|\ln(\Pi_+/\Pi_-)|$. The absolute value brackets are introduced into the expression, since the sign of the logarithm only indicates whether the relaxations proceed in a clockwise or counterclockwise direction. Table 3 lists the energies (in kcal) necessary to reach a steady state for the models here analyzed. Both for Ca^{2+} transport and for phosphorylase *b*, there is a good correspondence between the excess free energy liberated by the pseudoequilibrium and the free energy experimentally measured for the activity of the systems. This supports the validity of these simplified models for exploring the behavior of real systems.

Acknowledgements

This work was supported by the following grants: PHS-HL-13164, PHS-HL-33629, and PHS-DK-30322. Computer time and facilities were supported in part by the computer network of the University of Maryland at College Park and its branch at the Baltimore campus.

References

1 T.L. Hill, Free energy transduction in biology (Academic Press, New York, 1977).
2 D. Walz and S.R. Caplan, Proc. Natl. Acad. Sci. U.S.A. 84 (1987) 6152.
3 D. Walz and S.R. Caplan, Cell Biophys. 12 (1988) 13.
4 J. Wyman, Proc. Natl. Acad. Sci. U.S.A. 72 (1975) 3983.
5 G. Inesi, M. Kurzmack and D. Lewis, Methods Enzymol. 157 (1988) 154.
6 D.J. Graves and J.H. Wang, in: the Enzymes, ed. P.D. Boyer (Academic Press, New York, 1972) vol. 7, p. 435.
7 R.J. Fletterick and S.R. Sprang, Acc. Chem. Res. 13 (1982) 361.
8 R.F. Steiner, L. Greer and R. Bhat, Biochemistry 18 (1979) 1380.
9 P.L. Mateo, C. Baron, O. Lopez-Mayorga, J.S. Jimenez and M. Cortijo, J. Biol. Chem. 259 (1984) 9384.
10 M.H. Buc and H. Buc, in Regulation of enzyme activity and allosteric interactions, eds. E. Kvamme and A. Phil (Academic Press, New York, 1968) p. 109.